Asymmetric nonlinear conductance of quantum dots with broken inversion symmetry

H. Linke,* W. D. Sheng, A. Svensson, A. Löfgren, L. Christensson, H. Q. Xu, and P. Omling
Solid State Physics, Lund University, Box 118, S-22100 Lund, Sweden

P. E. Lindelof
Niels Bohr Institute, University of Copenhagen, Universitetsparken 5, DK-2100 Copenhagen, Denmark
(Received 8 September 1999)

Coherent electron transport in open, asymmetric (triangular) quantum dots is studied experimentally and theoretically in the nonlinear response regime. The nonlinear dot conductance is found to be asymmetric with respect to zero bias voltage. This conductance asymmetry is related to the nonsymmetric effect of an applied electric field on the quantum electron states inside the dot and on their coupling to the states in the electron reservoirs. The direction of the asymmetry depends sensitively on the amplitude of an applied ac voltage, on the Fermi energy and on the magnetic field, and is suppressed at temperatures above a few Kelvin. Quantum dots can therefore be viewed as ratchets, that is, devices in which directed particle flow is induced by nonequilibrium fluctuations, in the absence of (time-averaged) external net forces and gradients. A quantum mechanical model calculation reproduces the key experimental observations. The magnitude of the conductance asymmetry is found to depend strongly on the electric field distribution inside the dot. In addition to exact calculations, an approximation is presented which makes it possible to qualitatively predict the nonlinear behavior from the energy dependence of the conductance in the linear response regime. We also discuss a semiclassical explanation for our observations and comment on limits of quantum-interference induced rectification.

I. INTRODUCTION

The majority of studies of electron transport in mesoscopic systems has to date been limited to the linear response regime where effects of thermal nonequilibrium can be neglected. Small electronic systems at low temperatures, however, can easily be driven away from thermal equilibrium and nonlinear effects are therefore important already at small bias voltages.[1] The lowest order of nonlinearity, that is, the term G_1 in the expansion of the current $I=G_0U+G_1U^2+\ldots$, leads to the rectification of an external voltage U. In general terms, rectification can be defined as the directed motion of particles in asymmetric potentials in the absence of time-averaged macroscopic net forces. Devices in which the rectification of nonequilibrium fluctuations or fields can be observed are often called ratchets[2,3] and have in recent years attracted considerable interest in a broad physics community. This interest is in part of a fundamental nature but is also motivated by the prospect of applications. One field to which the physical concept of rectification in ratchets may be applicable is the chemomechanical energy conversion in biological cells. There, mechanical work is generated by so-called molecular motors in the absence of macroscopic forces or thermal gradients.[4–6] In these systems it is thought that the Brownian motion of molecules is rectified using energy from nonequilibrium chemical reactions.

The necessary conditions for rectification in any system are, first, a lack of central symmetry of the potential (thus defining a preferential direction of motion), and, second, a state of thermal nonequilibrium (rectification in thermal equilibrium would violate the second law of thermodynamics).[7,8] In a diode based on a *pn* junction or a Schottky barrier, for instance, the symmetry is broken by the doping profile or a band offset, respectively, and a state of thermal nonequilibrium is created by application of an electric field. Then, even if the applied field is zero on time-average, a directed current is generated. Another example is the photogalvanic effect, that is, the generation of current by illuminating a homogeneous but microscopically not centrosymmetric material.[7,8]

Mesoscopic semiconductor structures provide an almost ideal laboratory for studies on rectification, because today a large variety of fabrication techniques is available to create potentials of defined symmetry, or asymmetry, and electrical currents can be measured with extremely high accuracy. Most importantly, however, at low temperatures the electronic properties of mesoscopic structures are determined by quantum effects. Mesoscopic structures in the non-linear regime can therefore be used to study rectification due to quantum processes such as tunnelling[9–11] and quantum interference.[12] Such quantum rectification is the focus of the present paper. Specifically, we will present a detailed investigation of asymmetries in the nonlinear conductance of semiconductor quantum dots without spatial inversion symmetry (Fig. 1).

Quantum dots are two-dimensional electron cavities, usually of the order of 20 times larger than the electron Fermi wavelength, but much smaller than the electron mean free path for impurity scattering. At low temperatures transport through such structures is phase coherent and determined by the coupling of electron states in the reservoirs to the electron states inside the dot. The electrostatic potential that determines the electron states inside the dot can be modified by an electric field via point contacts. Therefore, the conductance of quantum dots depends on the applied voltage already at voltages as small as a few hundred microvolts, or a

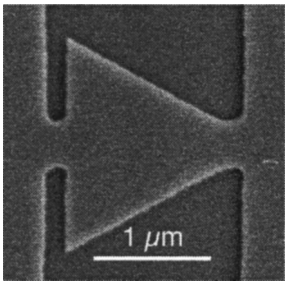

FIG. 1. Scanning electron micrograph of a triangular quantum dot as used in the present work. The structure was patterned using electron beam lithography and was transferred into GaAs/AlGaAs heterostructure material by shallow wet etching (etched areas are darker in the image). An additional top-gate made it possible to tune the electron concentration in the dot and surrounding areas.

few percent of the Fermi energy. If the geometry of the quantum dot is not symmetric with respect to the direction of the current, these nonlinear quantum effects depend, in general, on the direction of the electric field.[12–14] Consequently, asymmetric quantum dots can partly rectify an ac voltage applied over the structure. The direction of the net current depends on the exact configuration of the electronic states and can not be deduced from the orientation of the triangle in a straightforward way. Reversals of the direction of the rectified current can be observed as a function of ac voltage amplitude, Fermi energy or magnetic field. The key property of the dot that leads to rectification is, however, the broken symmetry of the shape of the dot, which is defined by the lithographic design of the device. This is in contrast to previous experiments using mesoscopic semiconductor structures in which the symmetry of the potential was broken because of the random distribution of impurities.[15–19]

In a recent article, rectification in triangular quantum dots (Fig. 1) was demonstrated, and it was shown that modeling of quantum transport in the nonlinear regime qualitatively accounts for the experimental observations.[12] Here, we present additional experimental results and carry their theoretical interpretation one step further. In Sec. II we will create a basis for the theoretical discussions by giving an overview of the main experimental results. After a description of the theoretical methods used we investigate the physical origin of the asymmetric conductance in Sec. III. One issue that will be raised is the relative importance of different quantum rectification mechanisms which could be essential in our device. Specifically, we distinguish the effect of the geometrical asymmetry of the dot and secondary effects related to the self-consistent, spatial distribution of an applied electric field. We will also present an intuitive understanding of the results based on the theory presented in Ref. 20 which expresses the nonlinear behavior of quantum dots derived from their energy-dependent conductance spectrum in the linear response regime. In Sec. IV, we compare the experimental and theoretical results and point to effects which are not currently included in the theoretical model. We present a semiclassical picture of nonlinear quantum transport in electron cavities and discuss classical rectification effects. Further, we discuss the limits of interference-induced rectification in open quantum dots. Finally, our results are summarized in Sec. V where also some open questions are addressed.

II. EXPERIMENT

A. Devices

The triangular quantum dots used in the present work were defined by electron beam lithography and shallow wet etching in modulation-doped, GaAs/$Al_xGa_{1-x}As$, two-dimensional electron gas material (Fig. 1). The transport properties of similar devices fabricated by the same process methods have been previously characterized in great detail in the linear response regime.[21,22] Here, we build on these earlier results and extend the studies into the nonlinear regime of transport. We will present data from one particular device, representative of data from in excess of fifteen different devices studied in the nonlinear response regime.

The effective, inner side length of the dot potential as determined from classical commensurability effects in magnetoresistance measurements[21] was about 1.7 μm, much less than the electron mean free path with respect to impurity scattering of about 15 μm. Using a top gate, the Fermi energy (μ_F, determined from Shubnikov–de Haas oscillations in an area outside the billiard) was tunable in the range 7–9 meV, corresponding to a Fermi wavelength (λ_F) of 0.05–0.06 μm. Typically four modes were open at the point contacts. Current controlled, two-terminal resistance measurements were carried out, using separate current and voltage probes in a four-point geometry, with an excitation voltage $U_{ac} < k_B T \approx 25\,\mu$eV. Unless otherwise indicated, the temperature was $T = 0.3$ K.

To study electron transport in the nonlinear regime, we measured the differential resistance $R = \partial U(I)/\partial I$ as a function of a dc bias current (I) which was added to the ac component used for lock-in detection. The differential conductance $G(U) = 1/R(U)$ was then calculated from the measured raw data, where U is the source-drain voltage.

B. Temperature and magnetic field dependence

In the present work we are interested in quantum rectifying effects, that is, in nonsymmetric effects that can be related to the nonlinear response of the quantum properties of the electron cavities being studied. Since nonlinear effects of a classical nature can also lead to rectification in asymmetric microstructures,[23,24] it is necessary to establish techniques which make it possible to experimentally distinguish classical and quantum effects. This distinction can be made because quantum and classical effects depend in different ways on temperature and magnetic field, as will be illustrated in the following.

In Fig. 2 we show measurements of the magnetoconductance of our triangular dot in linear response, that is, with no dc bias voltage applied. The bold and thin lines were recorded at $T = 0.3$ K and $T = 5$ K, respectively. It has been found previously, using devices processed in the same way as those studied here, that data recorded at the higher temperature can be explained in great detail in terms of commensurability effects due to a classical, billiard-ball-like motion of the electrons inside the cavity.[21] The quickly varying fluctuations emerging at the lower temperature, in contrast, are of quantum mechanical origin and can be interpreted in terms of variation in the density of states inside the billiard.[22] These quantum magnetoconductance fluctuations are observable only at very low temperatures (<1 K) where phase-

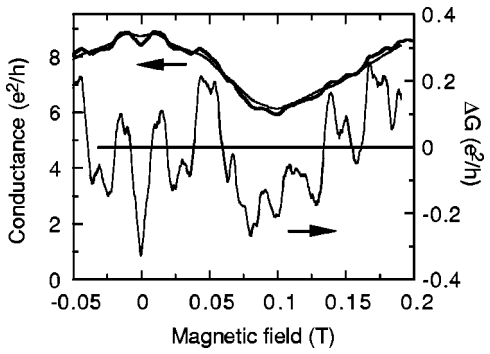

FIG. 2. Magnetoconductance of the triangular electron cavity (left axis) at $T=5$ K (thin line) and $T=0.3$ K (bold line). The conductance minimum at about $B=0.1$ T is caused by a classical commensurability effect (for details, see Ref. 21). By subtraction of the high temperature data from the low temperature data (shown with respect to the right-hand vertical axis) one can, to a good approximation, isolate the quantum conductance fluctuations, $\Delta G = [G(0.3\,\mathrm{K}) - G(5\,\mathrm{K})]$ (for details, see Ref. 22).

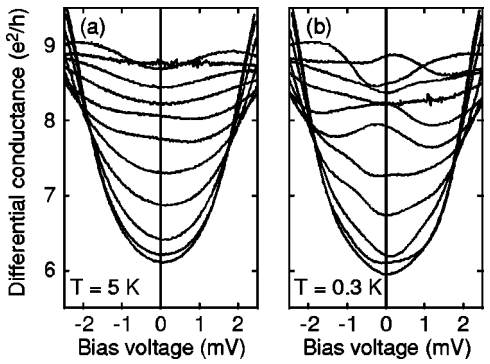

FIG. 3. (a) Differential conductance vs dc bias voltage U measured at a temperature of 5 K at, from the top down, magnetic fields between zero and 100 mT with a relative spacing of $\Delta B=10$ mT. The variation from curve to curve is associated with classical effects and the conductance values at $U=0$ agree with the magnetoconductance shown in Fig. 2. (b) When the temperature is lowered to 0.3 K additional structure emerges in the nonlinear conductance because of quantum interference effects.

destructive, inelastic electron scattering and thermal averaging are sufficiently suppressed. By subtracting the data recorded at the higher temperature from the low-temperature data, the quantum effects can be isolated to a good approximation (Fig. 2, right-hand axis). The rms value of the quantum fluctuations is about 0.15 e^2/h which is a typical value for experimentally observed magnetoconductance fluctuations at temperatures around 300 mK. The magnetic field scale (the correlation field B_C) of magnetoconductance fluctuations is given by the flux required to significantly change the electron states inside the cavity. Semiclassically, this field is given approximately by $B_C=(h/e)/a$, where a is the effective area of the device cavity (about 1.2 μm^2), which yields a value of a few millitesla for B_C, in agreement with Fig. 2. Classical effects, by comparison, change much more slowly with magnetic field, since the typical field scale here is determined by the field that markedly bends classical, ballistic electron orbits, i.e., when the cyclotron diameter becomes comparable to the lateral size of the device (about 100 mT for the present device).[21] These significant differences in the dependence on magnetic field and on temperature between classical and quantum behavior can be employed to distinguish classical and quantum effects also in the nonlinear response regime.

Measurements of the differential conductance as a function of the dc source-drain bias voltage are shown in Fig. 3, where the different curves have been recorded in a magnetic field range from 0 to 100 mT, at a relative separation of 10 mT. At $T=5$ K [Fig. 3(a)], when quantum effects are expected to be suppressed, the nonlinear conductance is in all cases found to increase monotonically with increasing bias voltage. The conductance value at zero bias voltage changes with magnetic field in agreement with Fig. 2 and the shape of the $G(U)$ curves depends qualitatively only little on magnetic field. At the lower temperature [$T=0.3$ K Fig. 3(b)], however, when quantum effects are expected to appear, the nonlinear behavior becomes more rich and varies qualitatively as a function of magnetic field. Following the same procedure as illustrated in Fig. 2 for the linear-response magnetoconductance we isolate the nonlinear quantum effects by subtracting the high temperature data from those recorded at low temperature (Fig. 4). In agreement with what one would expect for a quantum effect, the magnitude of the result is of the order of 0.1–0.2 e^2/h and depends strongly on the magnetic field. Most important, however, the nonlinear quantum effects are in general not symmetric with respect to zero bias voltage, where the orientation of the asymmetry depends on the magnetic field strength. It is this nonsymmetric quantum behavior that we will focus our attention on in the following. The slowly varying, classical, nonlinear effects, which are in general also slightly asymmetric, are not of primary interest here and will be commented on only briefly in Sec. IV.

The relative separation in magnetic field of the data sets shown in Fig. 4 ($\Delta B=10$ mT) is of the order of the scale of

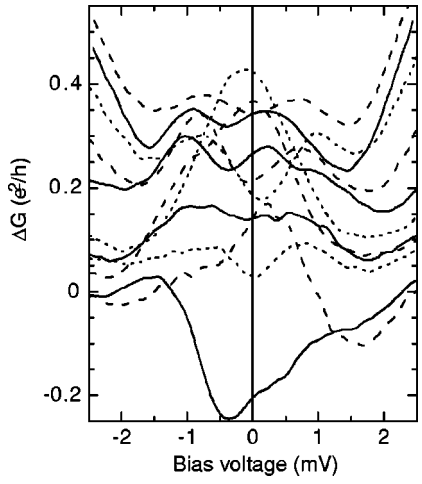

FIG. 4. The difference $\Delta G(U)=[G(U,T=0.3\,\mathrm{K})-G(U,T=5\,\mathrm{K})]$ at different magnetic fields between zero and 100 mT (relative spacing 10 mT), obtained by subtracting the data in Fig. 3(a) ($T=5$ K) from corresponding data in Fig. 3(b) ($T=0.3$ K). The curves have been offset by $+0.05$ e^2/h from one another and show, from the bottom up data for increasing magnetic field, where alternatingly full, long-dashed and short-dashed lines have been used. The curves were slightly smoothed to remove point-to-point noise occurring at the higher temperature.

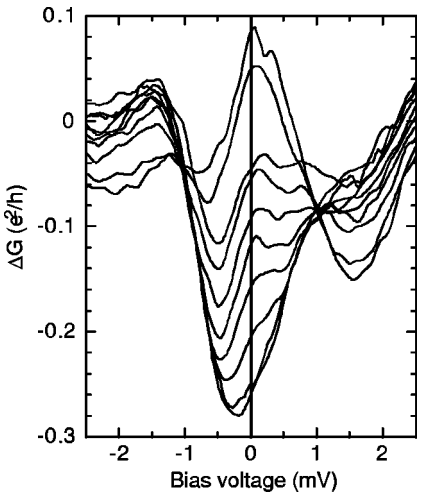

FIG. 5. The difference $\Delta G(U)=[G(U,T=0.3\,\mathrm{K})-G(U,T=5\,\mathrm{K})]$ obtained in the same way as the data shown in Fig. 4, but with a relative magnetic field spacing of only 1 mT. From the bottom up at the center of the graph, the magnetic field increases from zero to 9 mT.

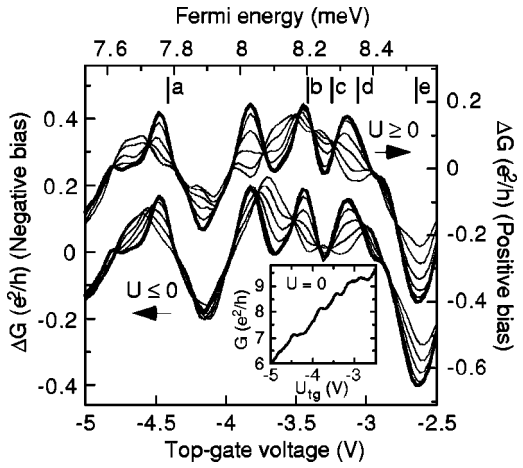

FIG. 6. Effect of a dc bias voltage on conductance fluctuations observed as a function of the Fermi energy (top axis) which was tuned using a top-gate (bottom axis). The lower (upper) group of plots have been recorded at increasing negative (positive) bias voltages and refer to the left-hand (right-hand) axis. The same absolute values of bias voltages have been used in both cases, namely $U=0$ (bold lines), ± 0.1 mV, ± 0.2 mV, . . . , ± 0.5 mV. These values for the voltage drop over the device refer to the center of the plot. Because the conductance depends on the Fermi energy, the effective voltage drop decreases by about 25% over the range of the graph. No magnetic field was applied. All data were obtained by subtracting a 2nd order polynomial fit from the raw data of $G(U_{tg})$. Inset: raw data of $G(U_{tg})$, recorded at zero bias voltage.

the correlation field B_C, which also significantly alters the linear-response conductance (Fig. 2), pointing to the same origin. In Fig. 5 we show data which have been obtained in the same way as those in Fig. 4, but with a relative separation of only 1 mT. With this higher resolution one can follow the evolution of the nonlinear behavior as a function of magnetic field, from an almost symmetric signal at zero magnetic field to a pronouncedly asymmetric shape at a few millitesla.

C. Fermi energy

The data presented in the previous section demonstrate a nonlinear, rectifying effect in asymmetric quantum dots which has the same magnitude, temperature dependence, and magnetic field dependence as magnetoconductance fluctuations observed in the linear response regime. We will show in the following that the relation between the observed, nonlinear behavior and the effect of an applied voltage on the electron states inside the electron cavity can be elucidated even better by using the Fermi energy as an experimental variable.

In the inset in Fig. 6 we show the conductance as a function of the top-gate voltage U_{tg} at zero magnetic field and zero bias voltage (linear response). Also indicated in Fig. 6 is the relation between U_{tg} and the Fermi energy, which was determined in the two-dimensional electron gas areas adjacent to the quantum dot, using Shubnikov–de Haas oscillations. The overall trend of the conductance to decrease with decreasing Fermi energy is due to the depletion of the point contacts, that is, due to the decreasing number of wave modes contributing to transport. Superposed on this slowly varying background are fluctuations which can be isolated by subtracting a second degree polynomial fit from the raw data (we have checked that this procedure yields, to a good approximation, the same outcome as subtraction of data measured at a higher temperature). The result is shown as bold lines in Fig. 6. The origin of these energy dependent fluctuations is similar to that of conductance fluctuations observed as a function of magnetic field (Fig. 2), i.e., these fluctuations reflect the oscillatory structure in the density of states inside the dot at zero magnetic field and the energy dependent coupling of the electron states to the reservoirs.

The effect of an electric field on the fluctuating (quantum) part of the dot conductance can be studied by measuring $G(\mu_F)$ at a series of bias voltages and subtracting the slowly varying background in the same manner as described above. Resulting data of $\Delta G(\mu_F)$ are shown in Fig. 6 for positive (right-hand axis) and negative bias voltages (left-hand axis), respectively, where the same absolute values of the bias voltages, $0<|U|<0.5\,\mathrm{mV}$, have been used in the two cases. Note that the bold lines in both groups of curves (zero bias voltage) are identical. From Fig. 6 it is immediately apparent that a bias voltage of the order of 0.5 mV modifies the conductance fluctuations as a function of the Fermi energy significantly. At certain energies these changes can be of the same magnitude (0.15 e^2/h) as the fluctuations themselves. Most importantly, these changes depend on the sign of the voltage, which becomes even more apparent when the positions of local maxima of $\Delta G(\mu_F)$ are plotted as a function of the Fermi energy and bias voltage (Fig. 7). Up to bias voltages of about $|U|\approx 1\,\mathrm{mV}$ one can follow the positions of individual maxima, which shift at a rate of typically $|d\mu_F/dU|\approx 0.1\,\mathrm{meV/mV}$. However, while some transmission resonances initially shift in a symmetric manner (for instance the peaks at $\mu_F=7.76\,\mathrm{meV}$ and 8.20 meV), the position of others is pronouncedly asymmetric with respect to zero bias voltage already at small voltages (e.g., at $\mu_F=8.04$ and 8.33 meV). At bias voltages $|U|>1$ mV the peak positions at corresponding negative and positive bias voltages are basically uncorrelated, that is, the electronic states inside the cavity are fully modified by the applied field.

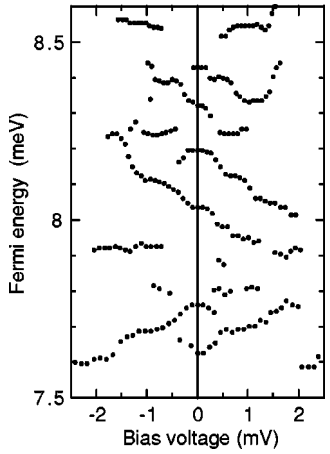

FIG. 7. Energy position of local maxima of conductance fluctuations, observed as a function of the Fermi energy for different dc bias voltages. The transmission resonances are shifted in a nonsymmetric manner by the applied electric field.

How the effect of an electric field on the transmission resonances, apparent in Figs. 6 and 7, manifests itself in the nonlinear conductance of the dot is illustrated in Fig. 8 where data of $G(U)$, recorded at different Fermi energies at $T=0.3\,\mathrm{K}$, are shown. The corresponding Fermi energies are marked with letters in Fig. 6.

To conclude this experimental section, the differential conductance of triangular electron cavities is, in the coherent regime of transport, in general not symmetric with respect to zero bias voltage. The observed asymmetry is clearly related to the asymmetric effect of an electric field on the electron states inside the cavity. In the following section we will present a quantum mechanical model calculation which accounts qualitatively for the observed quantum rectification.

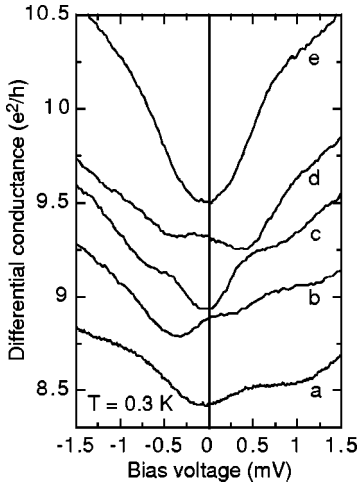

FIG. 8. Examples of the differential conductance versus bias voltage for different top-gate voltages. From the bottom up, $U_{tg}=-4.40,-3.44,-3.24,-3.08,-2.65$ V, corresponding to $\mu_F=7.79$, 8.20, 8.28, 8.35, 8.53 meV. The bottom curve has been offset by $+1.2\ e^2/h$. Note that in this plot the classical, nonlinear behavior has not been subtracted. Nonlinear quantum fluctuations are therefore less pronounced than it may appear in Fig. 6, where the quantum fluctuations have been isolated from the background.

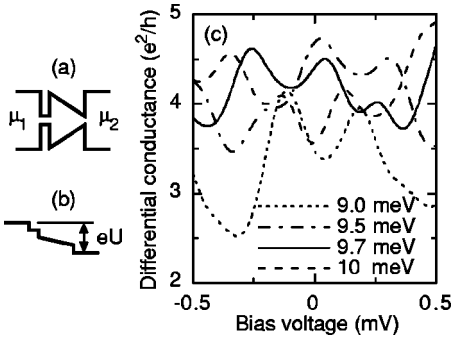

FIG. 9. (a) Geometry of the hard-wall potential used in the calculations. The side length of the equilateral triangle is 1 μm and the point contacts are 100 nm wide. (b) The assumed voltage drop distribution used (referred to as model I in the text). Potential steps are assumed at each discontinuity of the wave guide, and a linear slope is assumed inside the cavity where backscattering occurs. (c) Calculated differential conductance $G(U)$ for four different Fermi energies as indicated.

III. THEORY

The nonlinear regime of transport in mesoscopic systems has to date been addressed in only a limited number of theoretical studies. Büttiker and co-workers have developed a gauge-invariant theory for the frequency-dependent[25] and nonlinear[26] transport of mesoscopic systems, which takes the internal, self-consistent potential into consideration. So far, the application of Büttiker's nonlinear theory has been limited largely to studies of the lowest-order, nonlinear conductance in the weakly, nonlinear regime in quasi-one-dimensional[27] and two-dimensional[28,29] systems. In order to model our present experimental results, however, we wish not to be limited to the weakly nonlinear regime. We have therefore chosen to carry out exact numerical calculations of the differential conductance of a model potential in the nonlinear regime. We will show that the calculations yield qualitative agreement with the experimental results and we will discuss the physical origin of the quantum rectification mechanism. In particular, we will investigate the influence of the symmetry of the point contacts and of the geometrical shape of the cavity on quantum rectification.

A. Theoretical model

In our calculations we used a model potential that consists of an equilateral, triangular structure connected to two-dimensional electron reservoirs via two point contacts [Fig. 9(a)]. A hard-wall potential was used, which in previous studies was found to describe well the electronic properties of devices fabricated with the same hetereostructure material and by the identical processes as the ones used here.[21,22] The side length of the cavity was 1 μm, the largest size that was computationally feasible without reducing the accuracy of the calculation. The point contacts are 100 nm wide and support about four to five wave modes at the Fermi energies considered (9 to 10 meV). It is assumed that electron transport inside the cavity is ballistic and that any inelastic processes occur only far from the device. The reservoirs remain in local, thermal equilibrium at temperature T and their respective electrochemical potentials μ_1 and μ_2 are related to the applied source-drain voltage U by $\mu_1-\mu_2=eU$.

For calculations in the nonlinear regime of transport one needs to make assumptions about the profile of the electrostatic potential, which in general has a complicated dependence on the applied source-drain voltage. An exact determination of this dependence requires self-consistent treatment of the three-dimensional Schrödinger equation[30] and is beyond the scope of the present work. Several suggestions exist for simple assumptions on how the source-drain voltage drops between two reservoirs.[20,31–33] Here we adopt a convention[20] which was previously found to yield good agreement with the experiment of Ref. 34. A change in the electrostatic potential is assumed to be related to a probability for backscattering which occurs in our device inside the cavity and at each discontinuity of the potential or of the boundaries. As is shown in Fig. 9(b) we distribute one fourth of the potential drop eU linearly over the inside of the device, while the other three fourths of eU are dropped in equal parts abruptly at the discontinuities of the boundaries. This distribution of the voltage drop is in the following referred to as model I. In the present case these considerations lead to different total potential drops at the two point contacts. This is a result of the intrinsic asymmetry of the triangular structure, which makes it impossible to have two fully symmetric quantum point contacts attached to it.

If a Fermi-Dirac distribution $f(\varepsilon,T)$ is assumed for the electrons in the reservoirs, the total current through the device can be written as

$$I(U)=\int_0^\infty d\varepsilon\{f[\varepsilon-(\mu_F+eU),T]-f(\varepsilon-\mu_F,T)\}J(\varepsilon,U), \tag{1}$$

where $\mu_F=\mu_2$ was assumed and $J(\varepsilon,U)$ is the density of current, which can be calculated by scattering matrix methods.[35–37] In all calculations presented in the following the temperature $T=0.3\,\mathrm{K}$ was used. By definition, the differential conductance is given by $G(U)=\partial I(U)/\partial U$ which yields, in the limit of very small voltages, the linear response conductance. Calculations of the nonlinear differential conductance for four different Fermi energies are shown in Fig. 9(c). In all cases the differential conductance exhibits a complicated, nonmonotonic behavior. While the four datasets are quantitatively very different from one another, we note that all four of them are, on a scale of a few hundred microvolts, significantly nonsymmetric with respect to zero bias voltage. These observations are in qualitative agreement with the experimental results.

B. Origin of rectification and dependence on the voltage drop distribution

In order to understand the origin of the nonsymmetric effect it is helpful to discuss a simple model for transport through a quantum dot in the linear and nonlinear regime. First, we consider the case of negligible bias voltage [Fig. 10(a)]. Transport through the cavity is in this regime via the electron states within a few k_BT of the Fermi energy.[38] The states which contribute to transport are independent of the applied, very small voltage ($|eU|\ll k_BT$), and are the same for both current directions. This is the linear response regime where transport is by definition symmetric upon voltage reversal. For comparison, Fig. 10(b) shows the situation for finite bias voltage, that is, in the nonlinear response regime, using the voltage drop distribution of Fig. 9(b) (model I). One point to note here is that the assumed potential drop inside the electron cavity changes the potential landscape when the source-drain voltage is varied. Because of the nonsymmetric shape of the cavity, the resulting effective potential landscape depends also on the sign of the voltage. Therefore, the electron states which carry the current inside the dot depend on the absolute value and on the sign of the bias voltage, which leads to a nonlinear and nonsymmetric conductance. The second difference from the linear response regime is that at finite bias voltage not only electron states within a few k_BT of the Fermi energy contribute to transport through the dot. The contributing energy window is also determined by the voltage drop at the source quantum point contact. This will lead to rectification when the two point contacts are different, because a different range of quantized electron states will make a contribution at different signs of the voltage.

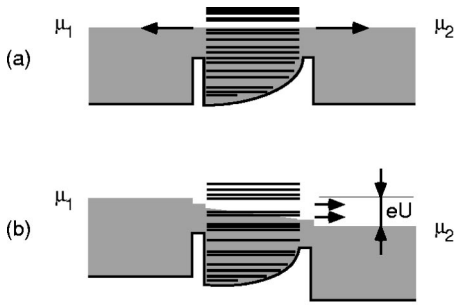

FIG. 10. Illustration of electron transport through a quantum dot. The curvature of the conductance band edge inside the dot represents the effect of the confinement energy inside the triangular dot (not to scale). The horizontal lines inside the dot indicate the shell structure of the density of states. The energy range $E<\mu$, where μ is the local electrochemical potential, is indicated by shading. (a) In linear response the transmission probability, that is, the conductance, is independent of the absolute value and the sign of the voltage. In (b) the energy diagram at finite voltage is shown, where a voltage drop distribution as in Fig. 9(b) (model I) has been used. This is the nonlinear response regime where the potential and the electron states depend on the voltage applied. The nonlinear conductance is asymmetric with respect to zero voltage when the potential is not inversion symmetric (see text).

The above discussion suggests that we can distinguish two sources of rectification in asymmetric quantum dots: The asymmetry of the scattering potential as a whole, and the nonidentical point contacts. We emphasize that these effects are related to one another, and can in reality not be separated. In the calculation, however, we have the freedom to make special assumptions concerning the potential distribution, allowing us to study the relative importance of each rectification mechanism.

First, we consider the effect of nonsymmetric point contacts and neglect the effect of a potential drop inside the dot. To achieve this, we use the potential distribution shown in the inset in Fig. 11(c) (model II). Two thirds and one third of the total voltage are assumed to drop at the left- and right-hand contact, respectively, while the potential in the interior of the dot remains flat. The resulting, nonlinear conductance is shown in Figs. 11(c) and 11(d) for two Fermi energies,

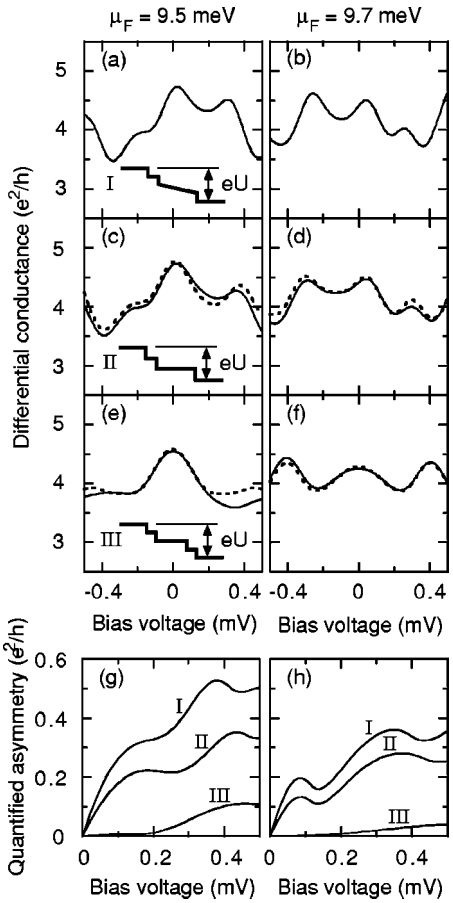

FIG. 11. (a)–(f) Calculated, differential conductance as a function of bias voltage for $\mu_F = 9.5$ meV (left-hand column) and $\mu_F = 9.7$ meV (right-hand column) ($T = 0.3$ K). Solid lines are exact calculations, dashed lines are approximations based on Eq. (3) (see text). From top, voltage drops according to models I, II, and III have been used as indicated [see insets to (a), (c), and (e), respectively]. The bottom figures (g) and (h) show the quantified asymmetries [Eq. (2)] of the exact calculations shown in panels (a)–(f).

$\mu_F = 9.5$ meV and $\mu_F = 9.7$ meV, respectively. Comparison with the data for model I [Figs. 11(a) and 11(b)] shows great qualitative similarity, although quantitatively the nonlinear conductance has changed. In order to compare the degree of non-symmetry for different models we define a quantified asymmetry

$$A(U) = \frac{1}{U}\int_0^U du\,|G(u) - G(-u)|, \tag{2}$$

which is the absolute value of the antisymmetric part of the differential conductance averaged over the voltage range $[0, \pm U]$. Data for $A(U)$ are shown in Figs. 11(g) and 11(h). It is worth noting that the asymmetry of the conductance is of the order of 0.5 e^2/h, which is in agreement with what one expects for an electron interference effect. Comparing the asymmetry of the conductance for voltage drop models I and II we note that their functional behavior is closely related, while the asymmetry for model I is consistently larger than that for model II. The same behavior was also found at all other Fermi energies investigated. We can therefore conclude that the removal of one source of non-symmetric behavior

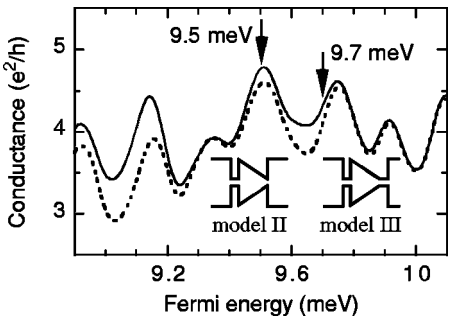

FIG. 12. Calculated, linear-response conductance (zero bias voltage) versus the Fermi energy for model II (solid line) and for model III (dashed line). The difference between the two models occurs because the point contact at the tip of the triangle was assumed in model III to be longer than in model II (see insets).

from model I, namely the voltage dependence of the potential inside the quantum dot, indeed reduces the asymmetry of the conductance. The next step will now be to artificially also remove from the calculation the non-symmetry of the voltage drop at the point contacts. To achieve this, the contact at the tip was in this calculation made longer to match the length of the base contact (see inset to Fig. 12), which results in the fully symmetric voltage drop shown as model III in Fig. 11. The only remaining asymmetry in this configuration is now the geometrical shape of the hard-wall potential which forms the dot itself. We emphasize again that we are here making a nonrealistic assumption: The symmetry of the voltage drop is related to the symmetry of the hard-wall potential, such that a symmetric voltage drop in a nonsymmetric structure is not meaningful. By retaining this assumption for the moment, however, we can investigate the effect of the shape of the dot alone, without any additional (self-consistently related) effect due to the electric field. The resulting, nonlinear conductance is shown in Figs. 11(e) and 11(f). Also in this case the conductance is found to be asymmetric, see Figs. 11(g) and 11(h), because also in this case the effective dot potential depends on the direction of the electric field, due to the spatial asymmetry of the dot. Nevertheless, the asymmetry for model III is significantly smaller than for models I and II. We have checked that the conductance of a fully symmetric (rectangular) dot yields a perfectly symmetric conductance, as is expected from symmetry arguments.

We can conclude from this discussion that rectifying effects induced by geometry are observed independent of the details of the voltage drop used in the calculation. In particular, the dot shape alone yields rectification also when the voltage drop used is fully symmetric [Figs. 11(e) and 11(f)]. Quantitatively, however, quantum rectification is significantly enhanced by the asymmetric distribution of the electron potential, which is a necessary consequence[1] of the dot geometry [Figs. 11(g) and 11(h)].

It should be noted that also model I, the most realistic one of the three models used here, does not consider all sources of nonsymmetry, because the spatial distribution of the electric field assumed there is symmetric upon voltage reversal. In general, however, the electric field distribution in a nonsymmetric structure will self-consistently also depend on the sign of the voltage, giving rise to additional nonsymmetric

behavior. Also inelastic scattering inside the dot, which is excluded from the present model, gives rise to additional rectification.[38]

C. The energy dependence and the approximative approach

After this quantitative study of quantum rectification we will in the following present a more intuitive way to understand the general behavior of the nonlinear conductance. We begin by noting that part of the nonlinear behavior of the dot conductance is related to the voltage dependence of the energy window in which electron states contribute to transport, that is, to the energy dependence of the transmission function [Fig. 10 and Eq. (1)]. At small voltages, when the electron states inside the dot are not strongly altered by the electric field, it is therefore possible to predict the nonlinear behavior from the energy dependence of the conductance in linear response. It was shown [20] that at very low temperature the nonlinear, differential conductance can be approximately written as

$$G(\mu_F,U)\approx\{(1-\alpha)G_0[\mu_F+(1-\alpha)eU] + \alpha G_0(\mu_F-\alpha eU)\} \quad (\mu_F>\alpha eU) \qquad (3)$$

where α is the portion of the voltage that drops at the right-hand contact and $G_0(\mu_F)=G(\mu_F,U=0)$ is the differential conductance in linear response.[20] Equation (3) indicates that nonlinearities of the current caused by the energy dependence of the transmission function can be approximated by the weighted average of the two zero bias conductances at $[\mu_F+(1-\alpha)eU]$ and $[\mu_F-\alpha eU]$.[20] Nonlinear effects caused by the field dependence of the potential landscape inside the dot are, however, not considered by this simple model. Independent of the field distribution inside the cavity, the resulting nonlinear conductance is therefore symmetric with respect to zero bias voltage when $\alpha=\frac{1}{2}$, that is, when the voltage drop at the two point contacts is the same, and nonsymmetric otherwise.

In Figs. 11(c)–11(f) we show calculations of the nonlinear differential conductance $G=\partial I/\partial U$ using the approximation Eq. (3) (dashed lines) in comparison to the exact calculations of Eq. (1) (full lines). The same Fermi energies and voltage drop distributions have been used for the two calculations. Here, the approximated calculations using Eq. (3) are based on exact, calculated data for $G_0(\mu_F,T=0.3\,\mathrm{K})$ as shown in Fig. 12. From Fig. 11 it is apparent that the approximation Eq. (3) reproduces all features of the exact solution qualitatively very well. The quantitative agreement between approximation and model is best at small voltages, as is to be expected. For model II, even the nonsymmetry of the conductance is reproduced by the approximation, while for model III, where symmetric voltage drops at the point contacts are assumed, the approximation yields a symmetric, nonlinear conductance. For the more realistic and complex potential distribution according to model I the approximation as given by Eq. (3) can not be used in the form given because in this case not all of the voltage drop occurs at the point contacts. In spite of this, the resemblance of the approximation for model II [dashed line in Figs. 11(c) and 11(d)] with the exact calculation for model I [Figs. 11(a) and 11(b)] is still remarkably good. Equation (3) can therefore be used to gain an intuitive understanding of the quantum dot conductance in the nonlinear regime.

Consider $G_0(\mu_F)$ in Fig. 12 (model II). In the vicinity of $\mu_F=9.5\,\mathrm{meV}$ the linear response conductance has a local maximum, decreases monotonically to approximately $9.5\pm0.1\,\mathrm{meV}$, and continues to decrease in both directions after passing local maxima. From Eq. (3) one would therefore expect also the nonlinear conductance to decrease monotonically until the larger of αeU and $(1-\alpha)eU$ reaches ±0.1 meV, and to continue then to decrease non-monotonically towards higher bias voltages. This expectation agrees well with the observed behavior of the nonlinear conductance for $\mu_F=9.5\,\mathrm{meV}$ as shown in Fig. 11(c): The conductance decreases towards positive and negative voltages with shoulders at about $U\approx+0.3\,\mathrm{mV}$ and at $U\approx-0.2\,\mathrm{mV}$. A similar analysis can be made for $\mu_F=9.7\,\mathrm{meV}$ [see Fig. 11(d)] $G_0(\mu_F)$ is, with respect to this energy value, pronouncedly non-symmetric, showing a local minimum at $\mu_F\approx9.65\,\mathrm{meV}$ and a local maximum at $\mu_F\approx9.75\,\mathrm{meV}$. Consequently, also the nonlinear conductance is strongly asymmetric already in the vicinity of zero bias voltage, and exhibits non-monotonic behavior at $U\approx\pm0.1\,\mathrm{mV}$.

Also the experimental, nonlinear differential conductance can to some degree be understood using the model Eq. (3). For instance, at the top-gate voltage $U_{tg}=-2.6\,\mathrm{V}$ (denoted by *e* in Fig. 6) where $G(\mu_F,U=0)$ exhibits a pronounced local minimum, also the nonlinear conductance shows a clear minimum around zero bias voltage (curve *e* in Fig. 8). A very detailed agreement of the approximation in Eq. (3) with experimental data of $G(U)$ is not expected, however, because the approximation does not consider modifications to the electron states inside the dot induced by an electric field, which in the experiment are clearly quite important already at small voltages (see Figs. 6 and 7).

IV. DISCUSSION

A. Comparison of experiment and theory

From the experimental and theoretical results presented in the previous sections a consistent picture of nonlinear quantum effects in asymmetric electron cavities emerges. In the experiment as well as in the calculations we find that the nonlinear conductance exhibits rich structure in the coherent regime and is in general asymmetric with respect to zero bias voltage. The origin of the nonlinear fluctuations is the effect of the applied voltage on the electron states inside the dot, and on the coupling of the states to the reservoirs via the point contacts. Consequently, the nonlinear effects, and thereby the properties of quantum rectification, depend on the Fermi energy or the magnetic field in a sensitive way. Here, the scale in energy (or magnetic field) on which the nonlinear behavior changes, is consistent with the corresponding scale of correlation energy (or correlation magnetic field) for conductance fluctuations observed in linear response. Also the magnitude of the quantified asymmetry is experimentally and in theory consistent with the corresponding amplitude of conductance fluctuations observed at zero bias voltage. The most important conclusion is, therefore, that our theoretical model can qualitatively account for the key experimental observations.

In the following we will discuss some quantitative differences between the experiment and the calculation. A general observation is that the calculated, nonlinear conductance shows overall stronger and more pronounced structure than the experimental data. This is apparent, for instance, from a comparison of Figs. 4 and 9(c). The difference in fluctuation magnitude is, however, expected, given that the magnitude of fluctuations in linear response as a function of the Fermi energy are much smaller in the experiment than in the calculations. The corresponding rms values are approximately 0.15 e^2/h for fluctuations in the experiment (Fig. 6) and 0.45 e^2/h in the calculations (Fig. 12). The most obvious reason for this difference is that phase breaking, which leads to broadening of the electron states, is not included in the calculation.

Broadening of electron states is likely to be responsible also for differences between experiment and theory in the period of the quantum fluctuations. In the case of the linear-response conductance fluctuations as a function of the Fermi energy, both experiment and calculation yield that the fluctuations have a period of about 0.1 meV (Figs. 6 and 12). This suggests that fast fluctuations are suppressed by broadening in the experimental case because in the larger experimental cavity (side length 1.7 μm compared to 1 μm in the calculation) the conductance should vary faster as a function of energy.

Our calculations do not reproduce the experimental feature that the differential conductance usually increases with increasing bias voltages (Figs. 3 and 8), which is regularly observed in electron cavities studied in the non-linear regime.[39,40] An overall increase of the conductance is expected for higher voltages in the calculations, where more modes in the point contacts can eventually open. It is possible that this behavior is masked in the theoretical data by the coherent fluctuations which are, relative to the total conductance, stronger than in the experimental case. In addition, it is likely that the slowly varying conductance is at least in part due to effects that are not included in the theory, such as current heating.[39] We will return to this point in Sec. IV C.

Another difference between experiment and theory is the maximum voltage range in which quantum fluctuations of the nonlinear conductance can be observed. In the experiment the magnitude of the fluctuations generally decreases with increasing voltage, and fluctuations are not observable at voltages beyond about 2 to 3 mV. This suppression of fluctuations may be caused by thermal energy averaging due to current heating,[41] and by phase breaking due to electron-electron interaction of non-equilibrium electrons.[39,40] Since inelastic effects are not included in our theoretical model, this limitation of the voltage range is not relevant to the calculation.

B. Semiclassical discussion

Only quantum mechanical treatment, such as we used it in the theory section, is fully adequate to model quantum rectification effects as we report them here. However, it has been shown that, in the linear response regime, a semiclassical, ''billiard-ball'' picture of electron transport is remarkably successful in explaining quantum transport properties of triangular ballistic cavities.[22,42,43] An interesting question is, therefore, whether there is a simple classical or semiclassical explanation also for the nonlinear quantum effects as they are discussed here.

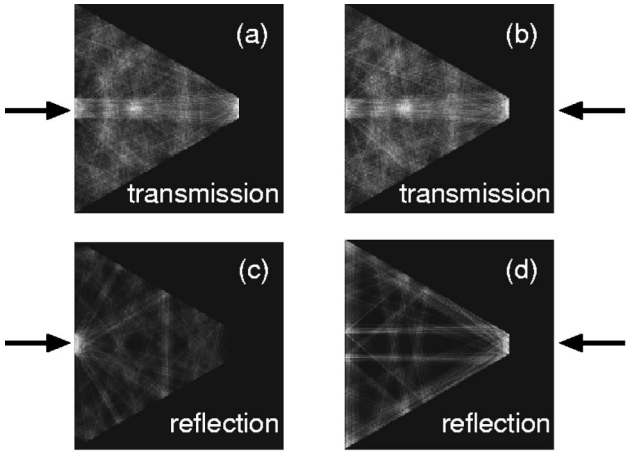

FIG. 13. Simulation of a large number of billiard-ball trajectories in a triangular electron billiard at $B=0$ (for details see text and Ref. 22). Left-hand (right-hand) figures: Electrons are injected via the contact in the side (tip), as indicated by the arrows. The lower figures show only the reflected trajectories and these depend on the direction of the injection. The transmitted trajectories (upper figures), however, which contribute to the current, are independent of the source contact. In thermal equilibrium, when direct and inversed states are equally populated, no rectification occurs. At finite voltages, however, when thermal equilibrium is disturbed, rectification can take place.

The billiard-ball picture of electron transport in thermal equilibrium is illustrated in Fig. 13. The figures on the left (right) show a superposition of a large number of simulated, classical trajectories of electrons which are injected into the billiard through the contact in the base of the triangle (tip). The same distribution of initial conditions has been used for both injection directions (for more details on the simulation technique, see Ref. 22). The upper (lower) two figures show only such trajectories that are transmitted (reflected) by the cavity. As one can intuitively expect, the reflected trajectories have an entirely different topography depending on the direction of injection [Figs. 13(c) and 13(d)], and one can be misled to assume that this difference causes rectification.[44] However, one must note that it is only the transmitted trajectories that contribute to the current. The striking, detailed agreement of the spatial distribution of transmitted trajectories in this simulation [Figs. 13(a) and 13(b)] illustrates why in thermal equilibrium no rectification occurs. The reason is that each trajectory that contributes to transport can be followed in either direction. In thermal equilibrium, when the occupation probability for direct and reversed electron momentum states (trajectories) is equal, it follows that equally many electrons will carry charge in either direction. This situation changes when thermal equilibrium is disturbed, for instance, by the application of a source-drain voltage (nonlinear response). Then, the transmitting trajectories will in general be occupied with different probabilities upon voltage reversal because electrons are nonisotropically accelerated in the applied electric field. Consequently, rectification occurs if the potential lacks central symmetry.[7] For a structure inverse to the one studied here, a triangular antidot, this clas-

sical, ballistic rectification mechanism has been discussed in detail[7,8] and was recently demonstrated experimentally in a ballistic microstructure.[23,24] Additional, classical, nonlinear effects are expected at higher voltages, where the scattering potential as a whole is altered by the applied field.

In the present report, however, we are concerned with a quantum mechanical effect. The common way to establish a semiclassical link between classical trajectories and quantum mechanical effects is to equip the classical paths with a phase and to include the possibility of electron interference.[45] In a situation where thermal equilibrium is disturbed by a bias voltage such that the occupation of transmitted trajectories depends on the current direction, also the interference between semiclassical electron paths will depend on the sign of the voltage. In addition to this effect, the interference of semiclassical electron paths depends in a sensitive way on the wavelength (energy) of the electrons involved. Analogous to our discussion of Fig. 10 (Sec. III) this energy dependence of the transmission probability will also lead to nonlinear effects. Therefore, at low temperatures, where transport through the dot is phase coherent, the classical, nonlinear behavior discussed above will have faster, nonsymmetric fluctuations related to electron interference superposed on it. This expectation is in agreement with our experimental observations, and we can conclude that the occurrence of quantum rectification can be anticipated using semiclassical arguments. Whether also a detailed understanding of quantum, nonlinear behavior can be gained, for instance, in terms of specific, classical electron trajectories, in the way this is possible for interference effects in triangular electron billiards in the linear response regime,[22,43] is a topic for future investigations.

C. Classical effects

In Sec. II we limited the discussion of our experimental data to quantum effects only. While it was possible to isolate the quantum behavior by subtracting data recorded at a higher temperature, it is clear from the preceding section that also nonlinear effects of an origin not related to electron interference can be expected in ballistic devices. That this is the case also in our devices is apparent from Fig. 3(a), where data recorded at 5 K are shown. At this temperature, where phase coherent effects are suppressed, the conductance is usually found to increase with bias voltage and is in general not fully symmetric with respect to zero bias voltage. As one would expect for a classical effect, the non-linear behavior varies only little upon small changes (a few millitesla) of the magnetic field. One reason for asymmetric, nonlinear behavior of classical origin may be the voltage dependence of the selection of classical trajectories as discussed above. In fact, strong effects of a bias voltage on classical commensurability effects in a magnetic field have been observed previously in triangular (see, for instance, Fig. 5 in Ref. 21) as well as rectangular[46] electron billiards, indicating that such effects will be important also here. A detailed understanding of nonlinear behavior in the classical regime is probably complicated. Nonlinear behavior of the point contacts,[47] current heating,[39,48] and electron-electron scattering of nonequilibrium electrons[21,46,49] may all be of importance.

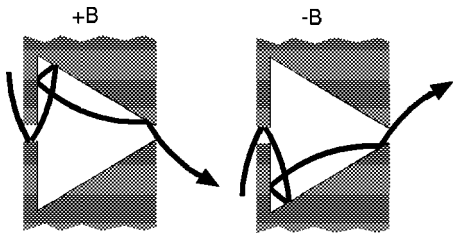

FIG. 14. Classical illustration of the symmetry of the nonlinear conductance in a magnetic field. The distribution of classical trajectories depends in the nonlinear regime on the direction of the current, and symmetry with respect to zero bias voltage is broken. The effect of a magnetic field, however, is independent of the direction of the magnetic field if the potential has a horizontal symmetry axis.

D. Is the symmetry of the dot geometry felt by the electrons?

So far we have restricted our discussion to the symmetry of conduction with respect to zero bias voltage. In this section we will consider the symmetry properties in a magnetic field as a tool to test the symmetry of the effective, real dot potential which is sampled by the electrons.

In the linear response regime, conduction is always symmetric with respect to zero magnetic field, that is, the relation $G(B)=G(-B)$ is valid independent of the potential symmetry.[38,50] For our device this is apparent from Fig. 2, where the linear response conductance is shown for positive and negative fields. In the nonlinear regime, however, when the conductance depends on the bias voltage, this general symmetry relation breaks down and symmetry in magnetic field is normally absent. It is restored only when the potential has a symmetry axis parallel to the direction of the current (Fig. 14). Under this condition, which is fulfilled in our dot geometry, the relation $G(U,B)=G(U,-B)$ is valid.

This symmetry relation allows us to perform an important test: if the reason for the absence of symmetry with respect to zero bias voltage is indeed the geometry of the dot (and not, for instance, broken symmetry because of random impurities of the material), then the conductance in the nonlinear regime should be symmetric with respect to zero mag-

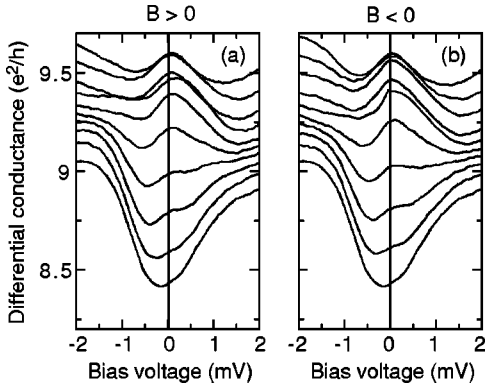

FIG. 15. Experimental data of the differential conductance $G(U)$ at increasing (a) positive and (b) negative magnetic field ($T=0.3$ K). The field values are, from the bottom up for (a) $B=-0.2,+1.8,+3.8,\ldots,+17.8$ mT and for (b) $B=-0.2,-2.2,-4.2,\ldots,-18.2$ mT (note the offset -0.2 mT of the magnetic field values, which is due to a residual field in the magnet). Each curve has been offset by $+0.1$ e^2/h from the preceding one.

netic field. Figures 15(a) and 15(b) show the nonlinear conductance at increasing positive as well as corresponding negative magnetic fields, respectively. Clearly, the nonlinear quantum conductance does not depend on the direction of the field within that field range which fully alters the nonlinear quantum fluctuations. We can therefore draw the conclusion that the effective dot potential does indeed have the symmetry properties that are apparent from Fig. 1, and that unintended deviations from this symmetry are not significant in the parameter range covered here ($|B|<20\,\mathrm{mT}, |U|<2\,\mathrm{mV}$). Therefore, the rectification observed can, indeed, be related to the intentionally asymmetric geometry of the dot.

E. Limits of geometry-induced quantum rectification

The triangular dot shape used in the present work is one of the simplest geometrical forms which lacks spatial inversion symmetry. It is therefore interesting to ask: would a different dot geometry generate even stronger quantum rectification? We can argue qualitatively that, at most, the nonlinear quantum fluctuations at negative and positive bias voltage can be fully uncorrelated. Then, the asymmetry Eq. (2) yields a value of the order of the magnitude of the quantum fluctuations themselves, that is, about 0.5 e^2/h rms at $T=0.3\,\mathrm{K}$ in our calculations (Fig. 12). This value can be compared to Figs. 11(g) and 11(h) where the averaged asymmetry according to Eq. (2) is shown. For model I, the asymmetry appears to level out at about 0.3 mV suggesting that no further increase of the quantum asymmetry occurs at higher voltages, and reaches values of about 0.5 e^2/h. One can therefore conclude that the triangular shape yields a quantum asymmetry close to the maximum that can be expected. At lower temperatures, when the fluctuation amplitude increases, larger total asymmetric effects can be observed, but one can not expect that the value of the asymmetry due to electron interference will exceed the order of the conductance unit e^2/h, independent of the dot geometry.

The situation may be different when the normalized asymmetry is considered, that is, the rectification coefficient $A(U)/G(U=0)$ which in the present case yields only a value of the order of a few percent. It is likely that this value can be increased by using a different geometry and fewer modes in the point contacts, thus decreasing the average conductance while keeping the asymmetry high.

Concerning the opposite limit of geometry-induced rectification it is of relevance to ask: What is the least geometrical asymmetry necessary to generate significant interference-induced rectification? One could argue that a minimum requirement is a nonsymmetric variation of the scattering potential on the scale of the Fermi wavelength because only then can the wave function spatially sample this variation. The rectification caused by such a small deviation from symmetry will, again, depend on the self-consistent field distribution, and is an issue for future investigations. Theoretical studies addressing this question may also clarify by how much the rectification properties of quantum dots are impaired by small imperfections of the effective, real dot potential, caused by individual impurities or process-related deviations from the intended dot shape.

V. SUMMARY

In the coherent, nonlinear regime of transport, asymmetric quantum dots exhibit conductance fluctuations which are not symmetric with respect to zero bias voltage. These nonlinear fluctuations occur because the electric field applied modifies the electron states inside the dot and the way these states couple to the states in the electron reservoirs via the quantum point contacts. Because of the broken symmetry of the dots, the nonlinear fluctuations are not symmetric and quantum rectification takes place.

The interpretation of our observations as a quantum mechanical effect is based on the experimental dependence of the nonlinear conductance fluctuations on the Fermi energy, on a small magnetic field, and on temperature, which are all in agreement only with an electron interference effect. Furthermore, the nonsymmetric conductance fluctuations can be related to the electric-field-induced shift and modification of transmission resonances which are known to be related to the quantum properties of the dot.

Quantum mechanical calculations of the conductance of a triangular dot confirm our interpretation and reproduce the key experimental results. The calculations depend on assumptions concerning the spatial distribution of the voltage drop over the device. While we find that qualitative agreement of the calculations with experiment is obtained independent of the details of the assumed voltage drop, there is a strong quantitative dependence of the strength of rectification on the exact electric-field distribution. In particular we find that even a fully symmetric voltage drop yields in the calculation a nonsymmetric conductance, simply because of the geometrical shape of the dot. More realistic models for the voltage drop must consider that the electric-field distribution will be nonsymmetric because it is self-consistently related to the symmetry of the scattering potential. Such nonsymmetric distributions of the voltage drop are found to substantially enhance the nonsymmetry of the conductance. Details of the nonlinear behavior at small voltages can be approximatively understood from the energy dependence of the linear-response conductance. One reason for quantitative differences between experiment and theory is that the calculations do not take effects of incoherence into account.

The occurrence of nonlinear conductance fluctuations can be understood also semiclassically, using a billiard-ball picture of electron transport combined with a quantum mechanical phase. It remains an intriguing, open question whether also a detailed semiclassical understanding of nonlinear effects in quantum dots can be obtained, such as is possible for interference effects observed in the linear response regime. Other open questions concern the limits of quantum rectification. On one hand, it is at present not clear what minimum geometrical asymmetry is required to produce observable, significant quantum rectification. On the other hand it is of fundamental and technological interest whether dot geometries exist that would yield rectification coefficients much larger than the value of a few percent observed here.

An important implication of our results is that asymmetric quantum dots can be viewed as quantum ratchets, that is, as devices that utilize a quantum effect to rectify nonequilibrium fluctuations.[12,51] Quantum dot ratchets have qualities not known from other rectifiers: For instance, the direction of

the rectified current is not related in a straightforward manner to the orientation of the dot, but depends sensitively on parameters such as the amplitude of the ac voltage, the Fermi energy and the magnetic field. These qualitatively new physical properties provide strong motivation for continued experimental studies of quantum ratchets.[9] Furthermore, motivation stems from potential, practical applications to so-called molecular motors in biological cells.[5] The extremely small physical size of molecular motors makes it likely that mesoscopic effects, such as electron tunneling or single charge effects, are of central importance for the operation of the motor. Mesoscopic devices and the theoretical models developed for mesoscopic semiconductor systems may therefore prove to be an ideal tool to significantly improve our understanding of molecular motors.

ACKNOWLEDGMENTS

The authors acknowledge helpful discussions with K.-F. Berggren, S. M. Reimann, and C. Pryor. This project was supported by the Swedish Research Councils for Natural and for Engineering Sciences, by the Göran Gustafsson Foundation for Research in Natural Sciences and Medicin, and by the Australian Research Council (HL). The authors thank Claus B. Sørensen and the III-V NANOLAB of MIC and NBI for the MBE-grown structures.

*Present address: School of Physics, The University of New South Wales, Sydney 2052, Australia. Electronic address: hl@phys.unsw.edu.au

[1] R. Landauer, in *Nonlinearity in Condensed Matter*, edited by A. R. Bishop, D. K. Campbell, P. Kumar, and S. E. Trullinger (Springer-Verlag, Berlin, 1987).

[2] R. P. Feynman, R. B. Leighton, and M. Sands, *The Feynman Lectures of Physics* (Addison-Wesley, Reading, 1963).

[3] P. Hänggi and R. Bartussek, in *Nonlinear Physics of Complex Systems—Current Status and Future Trends*, edited by J. Parisi, S. C. Müller, and W. Zimmermann (Springer, Berlin, 1996).

[4] M. O. Magnasco, Phys. Rev. Lett. **71**, 1477 (1993).

[5] F. Jülicher, A. Ajdari, and J. Prost, Rev. Mod. Phys. **69**, 1269 (1997).

[6] R. D. Astumian, Science **276**, 917 (1997).

[7] V. I. Belinicher and B. I. Sturman, Usp. Fiz. Nauk **130**, 415 (1980) [Sov. Phys. Usp. **23**, 199 (1980)].

[8] B. I. Sturman and V. M. Fridkin, *The Photovoltaic and Photorefractive Effects in Noncentrosymmetric Materials* (Gordon and Breach, Philadelphia, 1992).

[9] H. Linke, T. E. Humphrey, A. Löfgren, A. O. Sushkov, R. Newbury, R. P. Taylor, and P. Omling, Science **286**, 2314 (1999).

[10] P. Reimann, M. Grifoni, and P. Hänggi, Phys. Rev. Lett. **79**, 10 (1997).

[11] H. Q. Xu, Ann. Phys. (Leipzig) **8**, SI-289 (1999).

[12] H. Linke, W. D. Sheng, A. Löfgren, H. Q. Xu, P. Omling, and P. E. Lindelof, Europhys. Lett. **44**, 341 (1998).

[13] H. Linke, P. Omling, H. Q. Xu, S. M. Reimann, and P. E. Lindelof, in *Proceedings of the 23rd International Conference on the Physics of Semiconductors, Singapore, 1996*, M. Scheffler and R. Zimmermann (World Scientific, Singapore, 1996), p. 1593.

[14] H. Linke, Ph.D. thesis, Lund University, 1997.

[15] R. A. Webb, S. Washburn, and C. P. Umbach, Phys. Rev. B **37**, 8455 (1988).

[16] S. B. Kaplan, Surf. Sci. **196**, 93 (1988).

[17] P. A. M. Holweg, J. A. Kokkedee, J. Caro, A. H. Verbruggen, S. Radelaar, A. G. M. Jansen, and P. Wyder, Phys. Rev. Lett. **67**, 2549 (1991).

[18] D. C. Ralph, K. S. Ralls, and R. A. Buhrmann, Phys. Rev. Lett. **70**, 986 (1993).

[19] R. Taboryski, A. K. Geim, M. Persson, and P. E. Lindelof, Phys. Rev. B **49**, 7813 (1994).

[20] H. Q. Xu, Phys. Rev. B **47**, 15 630 (1993).

[21] H. Linke, L. Christensson, P. Omling, and P. E. Lindelof, Phys. Rev. B **56**, 1440 (1997).

[22] L. Christensson, H. Linke, P. Omling, P. E. Lindelof, K.-F. Berggren, and I. V. Zozoulenko, Phys. Rev. B **57**, 12 306 (1998).

[23] A. M. Song, A. Lorke, A. Kriele, J. P. Kotthaus, W. Wegscheider, and M. Bichler, Phys. Rev. Lett. **80**, 3831 (1998).

[24] A. M. Song, Phys. Rev. B **59**, 9806 (1999).

[25] M. Büttiker, A. Pretre, and H. Thomas, Phys. Rev. Lett. **70**, 4114 (1993).

[26] M. Büttiker, J. Phys.: Condens. Matter **5**, 9361 (1993).

[27] J. Wang, Q. Zheng, and H. Guo, Phys. Rev. B **55**, 9763 (1997).

[28] W. D. Sheng, J. Wang, and H. Guo, J. Phys.: Condens. Matter **10**, 5335 (1998).

[29] W. D. Sheng, Q. Zheng, J. Wang, and H. Guo, Phys. Rev. B **59**, 538 (1999).

[30] No report on self-consistent treatment of the electrostatic potential in a quantum dot in nonequilibrium has been available. For a theoretical treatment of this problem in the equilibrium case, see, for example, M. Stopa, Phys. Rev. B **54**, 13 767 (1996).

[31] L. I. Glazman and A. V. Khaetskii, Europhys. Lett. **9**, 263 (1989).

[32] C. S. Lent, S. Sivaprakasam, and D. J. Kirkner, Solid-State Electron. **32**, 1137 (1989).

[33] E. Castano and G. Kirczenow, Phys. Rev. B **41**, 3847 (1990).

[34] N. K. Patel, J. T. Nicholls, L. Martin-Moreno, M. Pepper, J. E. F. Frost, D. A. Ritchie, and G. A. C. Jones, Phys. Rev. B **44**, 13 549 (1991).

[35] H. Q. Xu, Phys. Rev. B **50**, 8469 (1994).

[36] H. Q. Xu, Phys. Rev. B **52**, 5803 (1995).

[37] W. D. Sheng, J. Phys.: Condens. Matter **9**, 8369 (1997).

[38] S. Datta, *Electronic Transport in Mesoscopic Systems* (Cambridge University Press, Cambridge, 1995).

[39] H. Linke, J. P. Bird, J. Cooper, P. Omling, Y. Aoyagi, and T. Sugano, Phys. Status Solidi B **204**, 318 (1997).

[40] H. Linke, J. P. Bird, J. Cooper, P. Omling, Y. Aoyagi, and T. Sugano, Phys. Rev. B **56**, 14 937 (1997).

[41] H. Linke, H. Q. Xu, A. Löfgren, W. Sheng, A. Svensson, P. Omling, P. E. Lindelof, R. Newbury, and R. P. Taylor, Physica B **272**, 61 (1999).

[42] M. Brack, J. Blaschke, S. C. Creagh, A. G. Magner, P. Meier, and S. M. Reimann, Z. Phys. D: At., Mol. Clusters **40**, 276 (1996).

[43] P. Bøggild, A. Kristensen, H. Bruus, S. M. Reimann, and P. E. Lindelof, Phys. Rev. B **57**, 15 408 (1998).

[44] The dependence of reflected trajectories on the injection direction illustrates the absence of detailed balance in spatially, not inversion-symmetric potentials. The lack of detailed balance leads to rectification when thermal equilibrium is disturbed, for

instance, by the application of an electric field. In thermal equilibrium, however, conduction remains symmetric according to the reciprocity principle. For a detailed discussion, see Ref. 8.

[45] M. Brack and R. K. Badhuri, *Semiclassical Physics* (Addison-Wesley, Reading, MA, 1997).

[46] L. Christensson, H. Linke, A. Löfgren, P. Omling, and P. E. Lindelof, Phys. Low-Dimens. Semicond. Struct. **1/2**, 253 (1998).

[47] L. P. Kouwenhoven, B. J. v. Wees, C. J. P. M. Harmans, J. G. Williamson, H. v. Houten, C. W. J. Beenakker, C. T. Foxon, and J. J. Harris, Phys. Rev. B **39**, 8040 (1989).

[48] L.-H. Lin, N. Aoki, K. Nakao, A. Andresen, C. Prasad, F. Ge, J. P. Bird, D. K. Ferry, Y. Ochiai, K. Ishibashi, Y. Aoyagi, and T. Sugano, Phys. Rev. B **60**, R16 299 (1999).

[49] T. Schäpers, M. Krüger, J. Appenzeller, A. Förster, B. Lengeler, and H. Lüth, Appl. Phys. Lett. **66**, 3603 (1995).

[50] M. Büttiker, Phys. Rev. Lett. **57**, 1761 (1986).

[51] P. Hänggi and P. Reimann, Phys. World **12**, 21 (1999); M. Brooks, New Scientist **2000**, 29.